5

Air Pollution Determination Using Remote Sensing Technique

H. S. Lim, M. Z. MatJafri, K. Abdullah and C. J. Wong
School of Physics, Universiti Sains Malaysia
11800 USM, Penang, Malaysia.

1. Introduction

Environmental pollution become more and more serious due to today's development all around the world. Environmental pollution is our concern nowadays because all the daily activities are related to the environment. In order to ensure this situation is under control, Malaysia's government has already established a network throughout Malaysia to monitor this situation. Air pollution is one of the most important environmental problems, which concentrates mostly in cities. Air pollution in Asian cities has grown with the progressing industrialization and urbanization. Air quality standards often refer to respirable suspended particulate matter (PM), being aerosols with a diameter smaller than 10 μm (PM10) (UNEP). Fine particles are of the greatest concern since they are capable of being easily transported over long distances on currents of air. Also, fine particles may be drawn into the respiratory airways where they may adversely affect health. Recently, the attention of scientists has been drawn towards studying the PM2.5 fraction and even smaller particles, which can penetrate the very deepest parts of the lung (Environmental Protection Service Tameside MBC Council Offices, 2008). The effects of environmental pollution in the study area are shown in Figure 1. The objective of air quality monitoring is to obtain an estimate of pollutant (total suspended particulates TSP) concentrations (Ung, et al., 2001a, 2001b). First, compared to atmospheric gases, aerosol is highly inhomogeneous and variable; that is, aerosol observations have to be global and continuous. Second, the available accuracy of aerosol characterization is often not sufficient. For instance, in situ measurements traditionally considered as the most reliable observations are inappropriate for global monitoring of aerosol radiative forcing parameters and usually do not characterize the aerosol in the total atmospheric column (Dubovik, et al., 2002).
Remote sensing has been widely used for environmental application such as for air quality and water quality studies. But the atmosphere affects satellite images of the Earth's surface in the solar spectrum. So, the signal observe by the satellite sensor was the sum of the effects from the ground and atmosphere. Tropospheric aerosols act to significantly alter the Earth's radiation budget, but quantification of the change in radiation is difficult because atmospheric aerosol distributions vary greatly in type, size, space and time (Penner, et al. 2002). Surface reflectance is a key to the retrieval of atmospheric components from remotely sensed data. Optical atmospheric effects may influence the signal measured by a remote

sensor in two ways: radiometrically and geometrically. This means that they can modify the signal's intensity through scattering or absorption processes and its direction by refraction (Sifakis and Deschamps, 1992).

The problem of particulate pollution in the atmosphere has attracted a new interest with the recent scientific evidence of the ill-health effects of small particles. Aerosol optical thickness in the visible (or atmospheric turbidity), which is defined as the linear integral of the extinction coefficient due to small airborne particles, can be considered as an overall air pollution indicator in urban areas (Sifakis, et al., 1998). Air pollution has long been a problem in the industrial nations of the West. It has now become an increasing source of environmental degradation in the developing nations of East Asia. The lack of detailed knowledge of the optical properties of aerosols results in aerosol being one of the largest uncertainties in climate forcing assessments. Monitoring of atmospheric aerosol is a fundamentally difficult problem. The problem of particulate pollution in the atmosphere has attracted a new interest with the recent scientific evidence of the ill-health effects of small particles. Air pollution is one of the most important environmental problems, which concentrates mostly in cities. Aerosols are liquid and solid particles suspended in the air from natural or man-made sources (Kaufman, et al., 1997).

The main objective of the present study is to test the performance of our proposed algorithm for mapping PM10 using Landsat satellite images. In situ measurements were needed for algorithm calibration. We used a DustTrak Aerosol Monitor 8520 to collect the in situ data. We collected the PM10 data simultaneously during the satellite Landsat overpass the study area. An algorithm was developed to determine the PM10 concentration on the earth surface. The efficiency of the proposed algorithm was determined based on the correlation coefficient (R) and root-mean-squares deviation, RMS. Finally, the PM10 map was generated using the proposed algorithm. In addition, the PM10 map was also geometrically corrected and colour-coded for visual interpretation.

(a)

Source: vincentchow, 2009

Source: The Digital Awakening-Haze in Penang

(b)

Source: The Digital Awakening-Haze in Penang Update - 10.48am

Fig. 1. Air pollution was found at (a) Kuching and (b) Penang, Malaysia

2. Remote Sensing

Remote sensing is a technique for collecting information about the earth without taking a physical sample of the earth's surface or touching the surface using sensors placed on a platform at a distance from it. A sensor is used to measure the energy reflected from the earth. This information can be displayed as a digital image or as a photograph. Sensors can be mounted on a satellite orbiting the earth, or on a plane or other airborne structure. Because of this energy requirement, passive solar sensors can only capture data during daylight hours. The major applications of remote sensing include environmental pollution, land cover/use mapping, urban planning, and earth management. We have to understand the basic concept of electromagnetic waves well enough for applying to the remote sensing techniques in our studies. We classify electromagnetic energy by its wavelength. This electromagnetic radiation gives an energy source to illuminate the target except the sensed energy that is being emitted by the target (Figure 2).

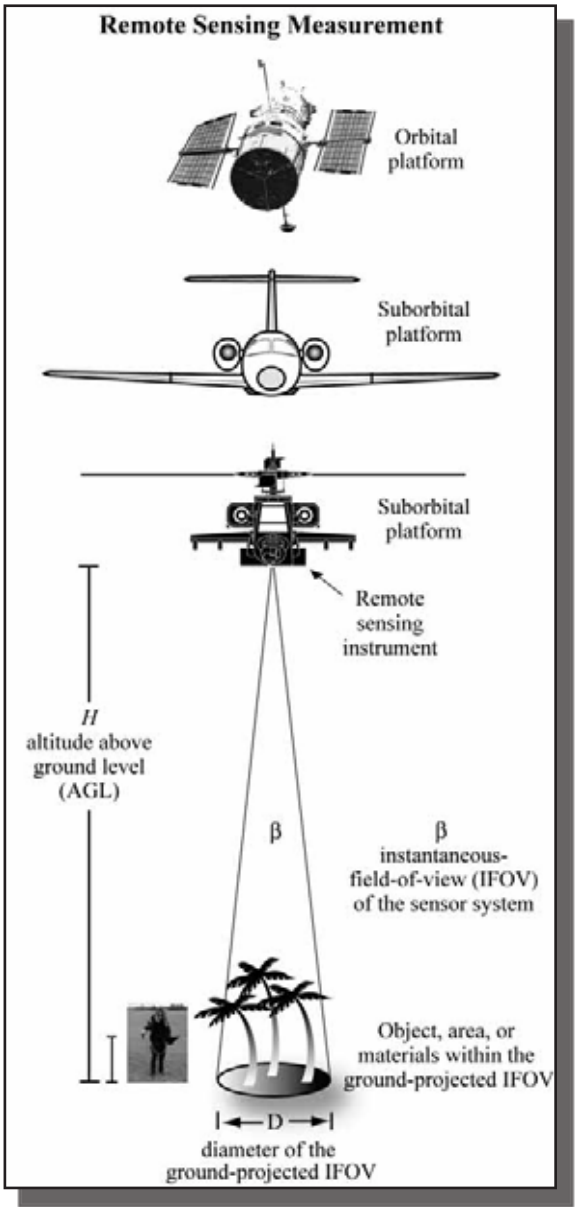

Fig. 2. Remote sensing instrument (Jensen, 2006)

There are two basic types of sensors: passive and active sensors (Figure 3). Passive remote sensors detect reflected energy from the sun back to the sensor; they do not emit energy itself. But active sensors can emit energy or provide its own source of energy and detect the reflected energy back from the target.

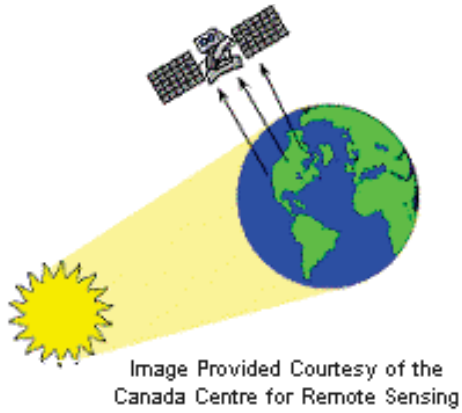

(a)

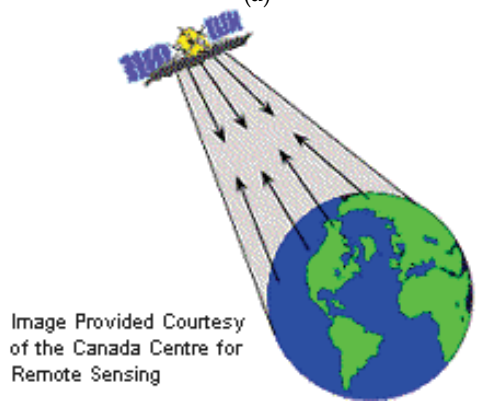

(b)

Fig. 3. (a) Passive sensor and (b) Active sensor (Fundamentals of Remote Sensing - http://www.ccrs.nrcan.gc.ca/resource/tutor/fundam/pdf/fundamentals_e.pdf.)

3. Study Area

The study area is the Penang Island, Malaysia, located within latitudes 5° 9′ N to 5° 33′ N and longitudes 100° 09′ E to 100° 30′ E. The map of the study area is shown in Figure 4. Penang Island is located in equatorial region and enjoys a warm equatorial weather the whole year. Therefore, it is impossible to get the 100 % cloud free satellite image over Penang Island. But, the satellite image chosen is less than 10 % of cloud coverage over the study area. Penang Island located on the northwest coast of Peninsular Malaysia.

Penang is one of the 13 states of the Malaysia and the second smallest state in Malaysia after Perlis. The state is geographically divided into two different entities - Penang Island (or "Pulau Pinang" in Malay Language) and a portion of mainland called "Seberang Perai" in Malay Language. Penang Island is an island of 293 square kilometres located in the Straits of Malacca and "Seberang Perai" is a narrow hinterland of 753 square kilometres (Penang-

Wikipedia, 2009). The island and the mainland are linked by the 13.5 km long Penang Bridge and ferry.

Penang Island is predominantly hilly terrain, the highest point being Western Hill (part of Penang Hill) at 830 metres above sea level. The terrain consists of coastal plains, hills and mountains. The coastal plains are narrow, the most extensive of which is in the northeast which forms a triangular promontory where George Town, the state capital, is situated. The topography of "Seberang Perai" is mostly flat. Butterworth, the main town in "Seberang Perai", lies along the "Perai" River estuary and faces George Town at a distance of 3 km (2 miles) across the channel to the east (Penang-Wikipedia, 2009).

The Penang Island climate is tropical, and it is hot and humid throughout the year. with the average mean daily temperature of about 27oC and mean daily maximum and minimum temperature ranging between 31.4°C and 23.5°C respectively. However, the individual extremes are 35.7°C and 23.5°C respectively. The mean daily humidity varies between 60.9% and 96.8%. The average annual rainfall is about 267 cm and can be as high as 624 cm (Fauziah, et al, 2006).

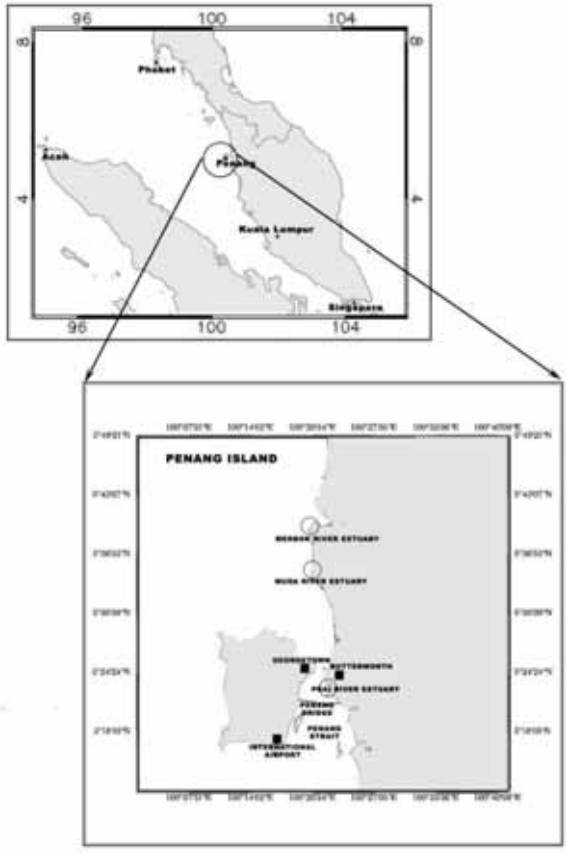

Fig. 4. The study area

4. Satellite Remote Sensing Data

For our research in USM, we use satellite images from passive sensors in our analysed. Images acquired by Landsat TM 5. On March 1, 1984, NASA launched Landsat 5 were used in this study, the agency's last originally mandated Landsat satellite. Landsat 5 was designed and built at the same time as Landsat 4 and carried the same payload: the Multispectral Scanner System (MSS) and the Thematic Mapper (TM) instruments.

Fig. 5. Landsat Satellite TM

5. Algorithm Model

The atmospheric reflectance due to molecule, R_r, is given by (Liu, et al., 1996)

$$R_r = \frac{\tau_r P_r(\Theta)}{4\mu_s \mu_v} \tag{1}$$

Where

τ_r = Rayleigh optical thickness

$P^r(\Theta)$ = Rayleigh scattering phase function

μ_v = Cosine of viewing angle

μ_s = Cosine of solar zenith angle

We assume that the atmospheric reflectance due to particle, Ra, is also linear with the τa [King, et al., (1999) and Fukushima, et al., (2000)]. This assumption is valid because Liu, et al., (1996) also found the linear relationship between both aerosol and molecule scattering.

$$R_a = \frac{\tau_a P_a(\Theta)}{4\mu_s \mu_v} \tag{2}$$

where

τ_a = Aerosol optical thickness

$P_a(\Theta)$ = Aerosol scattering phase function

Atmospheric reflectance is the sum of the particle reflectance and molecule reflectance, R_{atm}, (Vermote, et al., (1997).

$$R_{atm}=R_a+R_r \tag{3}$$

Where

R^{atm}=atmospheric reflectance
R_a=particle reflectance
R_r=molecule reflectance

$$R_{atm} = \left[\frac{\tau_a P_a(\Theta)}{4\mu_s \mu_v} + \frac{\tau_r P_r(\Theta)}{4\mu_s \mu_v} \right]$$

$$R_{atm} = \frac{1}{4\mu_s \mu_v} \left[\tau_a P_a(\Theta) + \tau_r P_r(\Theta) \right] \tag{4}$$

The optical depth is given by Camagni and Sandroni, (1983), as in equation (5). From the equation, we rewrite the optical depth for particle and molecule as equation (6)

$$\tau = \sigma \rho s \tag{5}$$

Where

τ = optical depth
σ = absorption
s = finite path

$$\tau = \tau_a + \tau_r$$ (Camagni and Sandroni, 1983)

$$\tau_r = \sigma_r \rho_r s \tag{6a}$$

$$\tau_p = \sigma_p \rho_p s \tag{6b}$$

Equations (6) are substituted into equation (4). The result was extended to a three bands algorithm as equation (7) Form the equation; we found that PM10 was linearly related to the reflectance for band 1 and band 2. This algorithm was generated based on the linear relationship between τ and reflectance. Retalis et al., (2003), also found that PM10 was linearly related to τ and the correlation coefficient for linear was better that exponential in their study (overall). This means that reflectance was linear with PM10. In order to simplify the data processing, the air quality concentration was used in our analysis instead of using density, ρ, values.

$$R_{atm} = \frac{1}{4\mu_s \mu_v}\left[\sigma_a \rho_a s P_a(\Theta) + \sigma_r \rho_r s P_r(\Theta)\right]$$

$$R_{atm} = \frac{s}{4\mu_s \mu_v}\left[\sigma_a \rho_a P_a(\Theta) + \sigma_r \rho_r P_r(\Theta)\right]$$

$$R_{atm}(\lambda_1) = \frac{s}{4\mu_s \mu_v}\left[\sigma_a(\lambda_1) P P_a(\Theta, \lambda_1) + \sigma_r(\lambda_1) G P_r(\Theta, \lambda_1)\right]$$

$$R_{atm}(\lambda_2) = \frac{s}{4\mu_s \mu_v}\left[\sigma_a(\lambda_2) P P_a(\Theta, \lambda_2) + \sigma_r(\lambda_2) G P_r(\Theta, \lambda_2)\right]$$

$$P = a_0 R_{atm}(\lambda_1) + a_1 R_{atm}(\lambda_2) \tag{7}$$

Where

P = Particle concentration (PM10)
G = Molecule concentration
R_{atmi} = Atmospheric reflectance, i = 1 and 2 are the band number
a_j = algorithm coefficients, j = 0, 1, 2, … are then empirically determined.

6. Data Analysis and Results

Remote sensing satellite detectors exhibit linear response to incoming radiance, whether from the Earth's surface radiance or internal calibration sources. This response is quantized into 8-bit values that represent brightness values commonly called Digital Numbers (DN). To convert the calibrated digital numbers to at-aperture radiance, rescaling gains and biases are created from the known dynamic range limits of the instrument.

$$\text{Radiance, } L(\lambda) = \text{Bias}(\lambda) + [\text{Gain}(\lambda) \times \text{DN}(\lambda)] \tag{8}$$

where
λ = band number.
L is the radiance expressed in $Wm^{-2}\ sr^{-1}\mu m^{-1}$.

The spectral radiance, as calculated above, can be converted to at sensor reflectance values.

$$\rho^* = \frac{\pi L(\lambda) d^2}{E_0(\lambda)\cos\theta} \tag{9}$$

Where

ρ* = Sensor Reflectance values
L (λ) = Apparent At-Sensor Radiance (Wm-2 sr-1μm-1)
d = Earth-Sun distance in astronomical units
= {1.0-0.016729cos [0.9856(D-4)]} where (D = day of the year)
E0 (λ) = mean solar exoatmospheric irradiance (Wm-2 μm-1)
θ = solar Zenith angle (degrees)

The rescaling gain and offset values for Landsat TM 5 used in this paper are listed in Table 1 (Chander, et al. 2007) and Solar Exoatmospheric spectral irradiances are given in Table 2 (Chander and Markham, 2003).

Landsat TM 5								
Rescaling Gain and Bias								
Processing Date	Mar 1, 1984 - May 4, 2003		May 5, 2003 - Apr 1, 2007		Apr 2, 2007 – Present			
Acquisition Date	Mar 1, 1984 - May 4, 2003		May 5, 2003 - Apr 1, 2007		Mar 1, 1984 - Dec 31, 1991		Jan 1, 1992 - Present	
Band	Gain	Bias	Gain	Bias	Gain	Bias	Gain	Bias
1	0.602431	-1.52	0.762824	-1.52	0.668706	-1.52	0.762824	-1.52
2	1.175100	-2.84	1.442510	-2.84	1.317020	-2.84	1.442510	-2.84
3	0.805765	-1.17	1.039880	-1.17	1.039880	-1.17	1.039880	-1.17
4	0.814549	-1.51	0.872588	-1.51	0.872588	-1.51	0.872588	-1.51
5	0.108078	-0.37	0.119882	-0.37	0.119882	-0.37	0.119882	-0.37
6	0.055158	1.2378	0.055158	1.2378	0.055158	1.2378	0.055158	1.2378
7	0.056980	-0.15	0.065294	-0.15	0.065294	-0.15	0.065294	-0.15

Table 1. Rescaling gains and biases used for the conversion of calibrated digital numbers to spectral radiance for Landsat TM 5

Unit: ESUN = $Wm^{-2}\mu m^{-1}$	
Band	Landsat TM 5
1	1957
2	1826
3	1554
4	1036
5	215.0
7	80.67

Table 2. Solar Exoatmospheric spectral irradiances in $Wm^{-2}\ \mu m^{-1}$ for Landsat TM 5

Landsat TM satellite data set was selected corresponding to the ground truth measurements of the pollution levels. The PCI Geomatica version 10.1 image processing software was used in all the analyses. The Landsat TM 5 satellite images were acquired on 15th February 2001 (Figure 6), 17th January 2002 (Figure 7), 6th March 2002 (Figure 8) and 5th February 2003 (Figure 9).

Raw digital satellite images usually contain geometric distortion and cannot be used directly as a map. Some sources of distortion are variation in the altitude, attitude and velocity of the sensor. Other sources are panoramic distortion, earth curvature, atmospheric refraction and relief displacement. So, to correct the images, we have to do geometric correction. After applying the correction, the digital data can then be used for other processing steps (Anderson, et al. 1976). Image rectification was performed by using a second order polynomial transformation equation. The images were geometrically corrected by using a nearest neighbour resampling technique. Sample locations were then identified on these geocoded images. Regression technique was employed to calibrate the algorithm using the satellite multispectral signals.

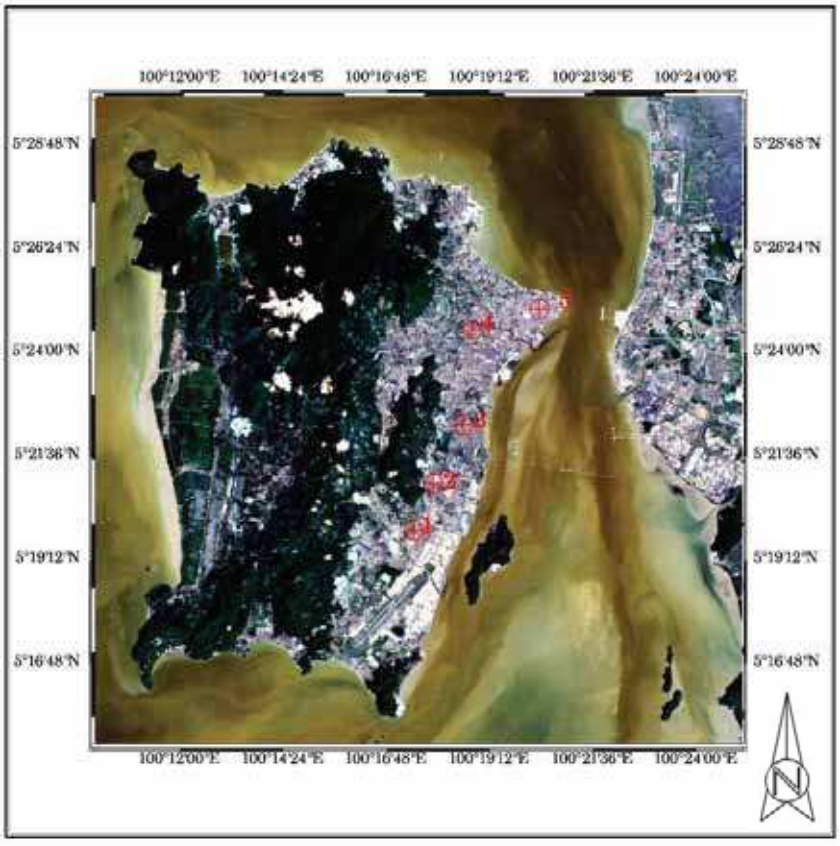

Fig. 6. Raw Landsat TM satellite image of 15th February 2001

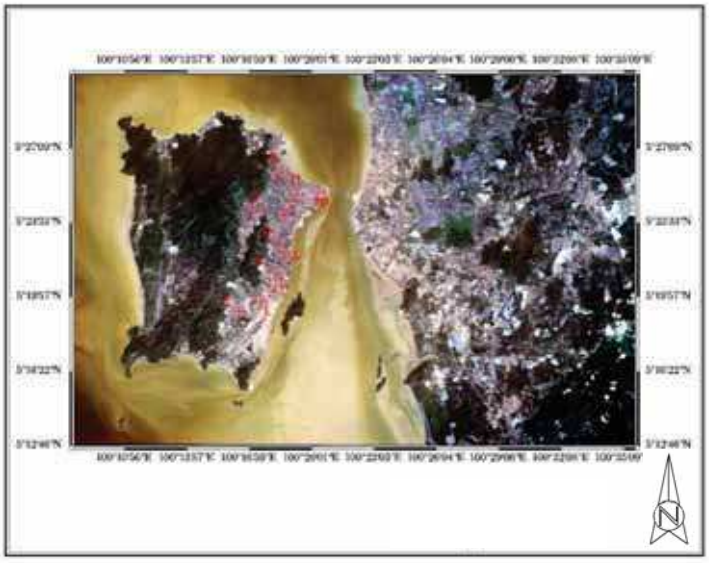

Fig. 7. Raw Landsat TM satellite image of 17th January 2002

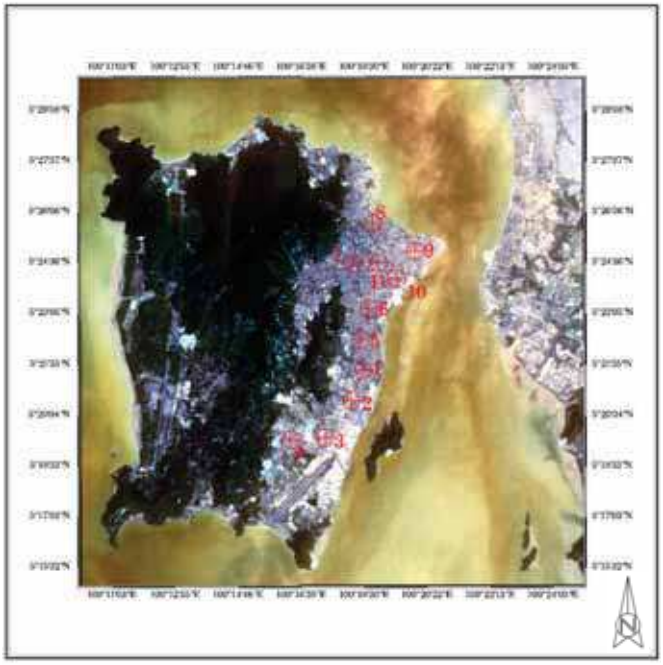

Fig. 8. Raw Landsat TM satellite image of 6th March 2002

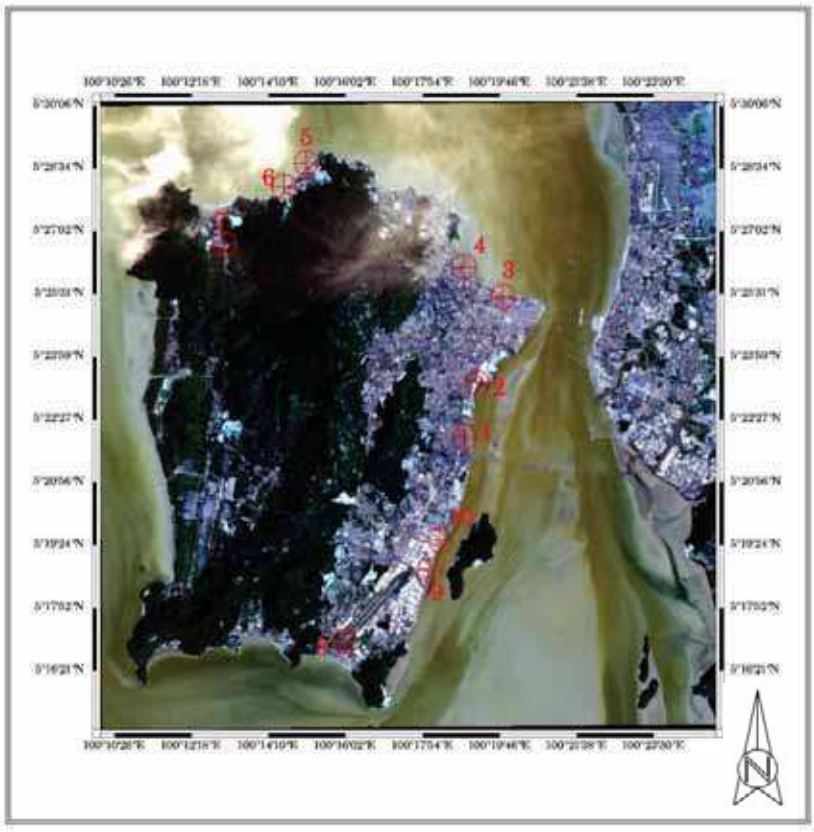

Fig. 9. Raw Landsat TM satellite image of 5th February 2003

It should be noted that the relfectance values at the top of atmospherr is the sum of the surface reflectance and atmospheric relfectance. The signals measured in each of these visible bands represent a combination of surface and atmospheric effects, usually in different proportions depending on the condition of the atmosphere. Therefore, it is required to determine the surface contribution from the total reflectance received at the sensor. In this study, we extracted the surface reflectance from mid-infrared band because the surface reflectance at various bands across the solar spectrum are correlated to each other to some extended. The surface reflectances of dark targets in the blue and red bands were estimated using the measurements in the mid-infrared band (Quaidrari and Vermote, 1999). Over a simple black target, the observed atmospheric reflectance is the sum of reflectance of aerosols and Rayleigh contributions (Equation 10). This simplification, however, is not valid at short wavelengths (less than 0.45 pm) or large sun and view zenith angles (Vermote and Roger, 1996). In this study, a simple form of the equation was used in this study (Equation 11). This equation also used by other research in their study (Popp, 2004).

$$R_s - TR_r = R_{atm} \quad (10)$$
$$R_s - R_r = R_{atm} \quad (11)$$

where:

Rs = reflectance recorded by satellite sensor
Rr = reflectance from surface references
Ratm = reflectance from atmospheric components (aerosols and molecules)
T = transmittance

It should be noted that the relfectance values at the top of atmosphere was the sum of the surface reflectance and atmospheric relfectance. In this study, we used ATCOR2 image correction software in the PCI Geomatica 9.1 image processing software for creating a surface reflectance image. And then the reflectance measured from the satellite [reflectance at the top of atmospheric, ρ(TOA)] was subtracted by the amount given by the surface reflectance to obtain the atmospheric reflectance. And then the atmospheric reflectance was related to the PM10 using the regression algorithm analysis (Equation 7). In this study, Landsat TM signals were used as independent variables in our calibration regression analyses. The atmospheric reflectances for each band corresponding to the ground-truth locations were determined. The atmospheric reflectance were determined for each band using different window sizes, such as, 1 by 1, 3 by 3, 5 by 5, 7 by 7, 9 by 9 and 11 by 11. In this study, the atmospheric reflectance values extracted using the window size of 3 by 3 was used due to the higher correlation coefficient (R) with the ground-truth data. The extracted atmospheric reflectance values were regressed with their respective ground -truth data and the proposed algorithm to obtain the regression coefficients. PM10 maps for all the images were then generated using the proposed calibrated algorithm and filtered by using a 3 x 3 pixel smoothing filter to remove random noise.
The data points were then regressed to obtain all the coefficients of equation (7). Then the calibrated algorithm was used to estimate the PM10 concentrated values for each image. The proposed model produced the correlation coefficient of 0.8 and root-mean-square error 16 $\mu g/m^3$. The PM10 maps were generated using the proposed calibrated algorithm. The generated PM10 map was colour-coded for visual interpretation [Landsat TM 5 - 15th February 2001 (Figure 10), 17th January 2002 (Figure 11), 6th March 2002 (Figure 12) and 5th February 2003 (Figure 13)]. Generally, the concentrations above industrial and urban areas were higher compared to other areas.

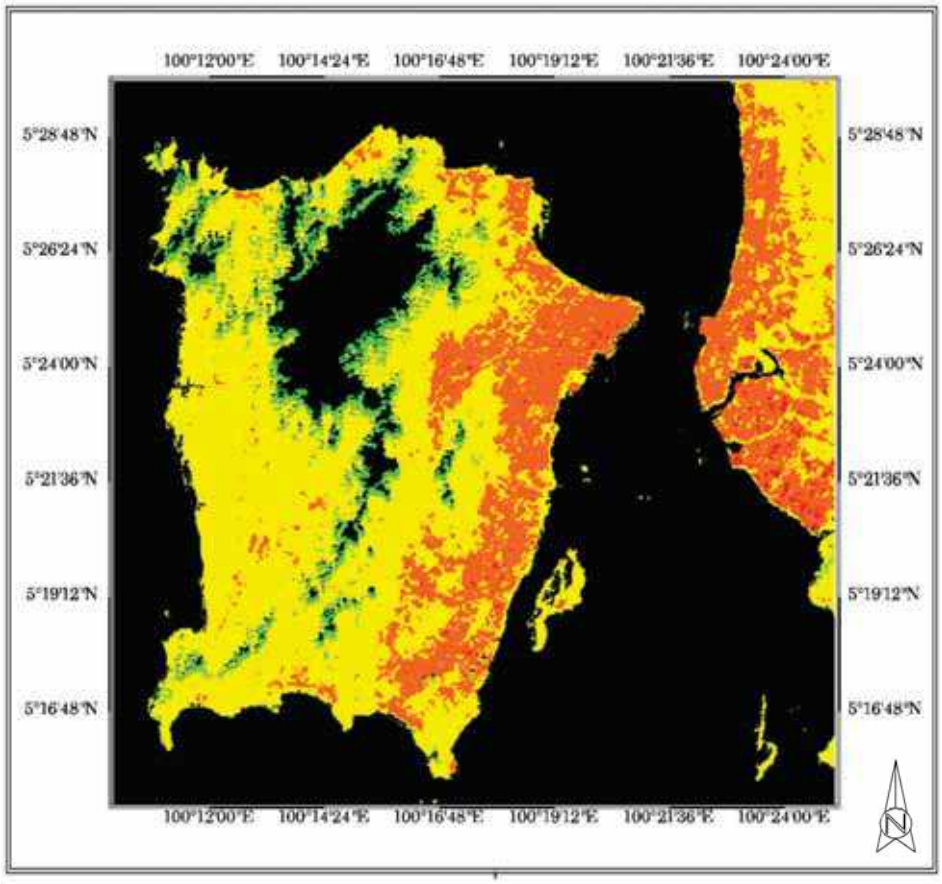

Fig. 10. Map of PM10 around Penang Island, Malaysia-15/2/2001 (Blue < 40 µg/m^3, Green = (40-80) µg/m^3, Yellow = (80-120) µg/m^3, Orange = (120-160) µg/m^3, Red = (>160) µg/m^3 and Black = Water and cloud area)

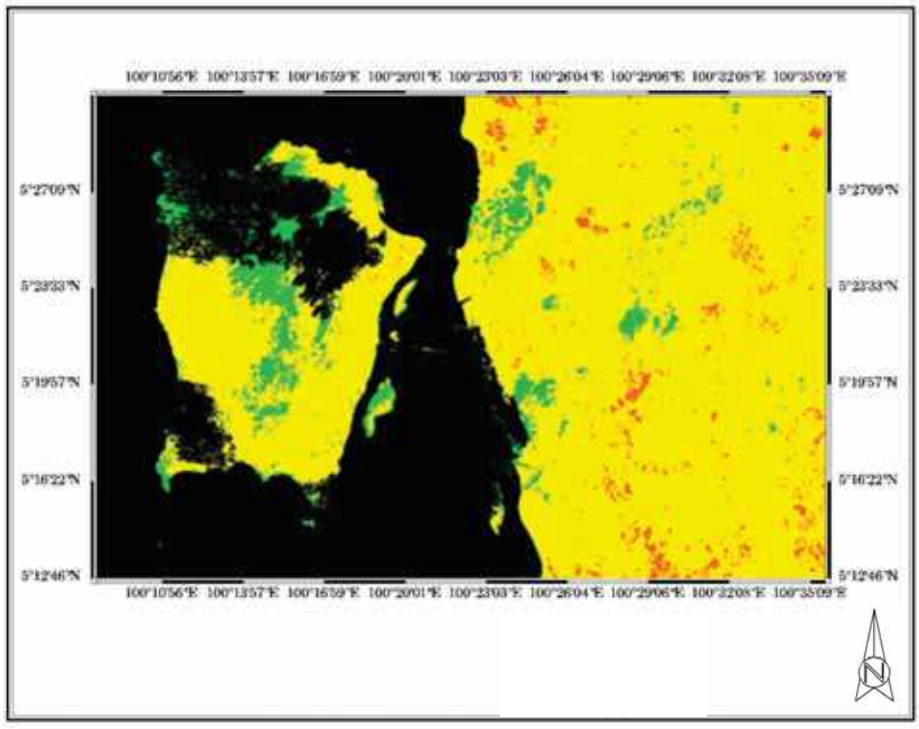

Fig. 11. Map of PM10 around Penang Island, Malaysia-17/1/2002 (Blue < 40 μg/m^3, Green = (40-80) μg/m^3, Yellow = (80-120) μg/m^3, Orange = (120-160) μg/m^3, Red = (>160) μg/m^3 and Black = Water and cloud area)

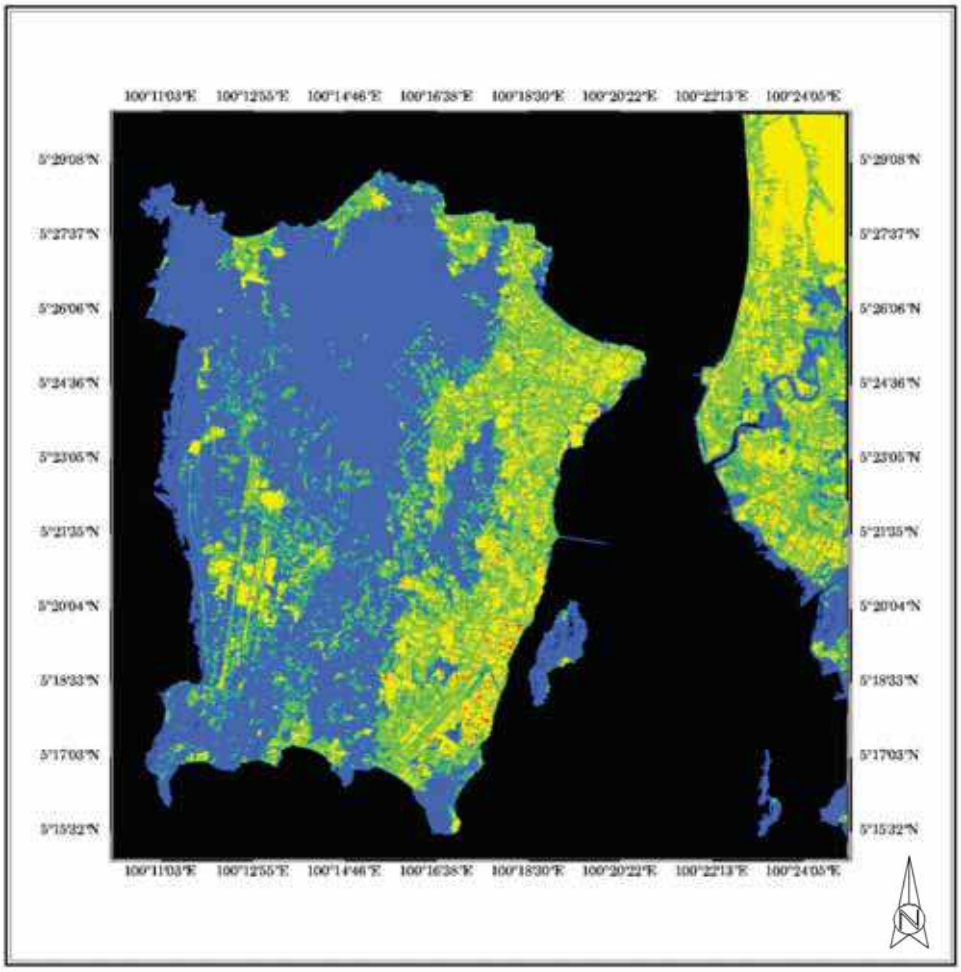

Fig. 12. Map of PM10 around Penang Island, Malaysia-6/3/2002 (Blue < 40 μg/m^3, Green = (40-80) μg/m^3, Yellow = (80-120) μg/m^3, Orange = (120-160) μg/m^3, Red = (>160) μg/m^3 and Black = Water and cloud area)

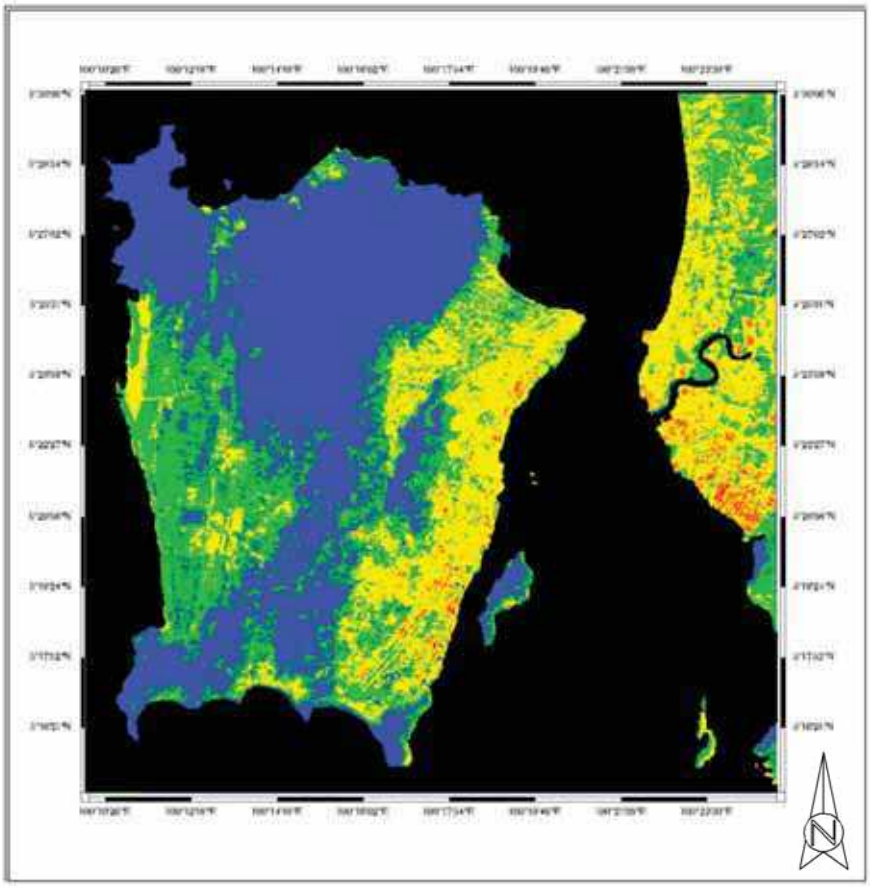

Fig. 13. Map of PM10 around Penang Island, Malaysia-5/2/2003 (Blue < 40 μg/m^3, Green = (40-80) μg/m^3, Yellow = (80-120) μg/m^3, Orange = (120-160) μg/m^3, Red = (>160) μg/m^3 and Black = Water and cloud area)

7. Conclusion

This study indicates that Landsat TM satellite data can provide very useful information for estimating and mapping air pollution. The proposed algorithm is considered superior based on the values of the correlation coefficient, R=0.8 and root-mean-square error, RMS=16 μg/m^3. This technique has been proved to be reliable and cost effective for such environmental study. Further study will be carried out to verify the results.

8. Acknowledgements

This project was supported by the Ministry of Science, Technology and Innovation of Malaysia under Grant 06-01-05-SF0298 " Environmental Mapping Using Digital Camera Imagery Taken From Autopilot Aircraft.", and also supported by the Universiti Sains Malaysia under short term grant " Digital Elevation Models (DEMs) studies for air quality retrieval from remote sensing data". We would like to thank the technical staff who participated in this project. Thanks are also extended to USM for support and encouragement.

9. References

Camagni. P. & Sandroni, S. (1983). Optical Remote sensing of air pollution, Joint Research Centre, Ispra, Italy, Elsevier Science Publishing Company Inc

Dubovik.; O., Holben, B.; Eck, T. F.; Smirnov, A.; Kaufman, Y. J.; King, M. D.; Tanre, D. & Slutsker, I. (2002). Variability of absorption and optical properties of key aerosol types observed in worldwide locations, American Meteorological Society, 590 – 608

Environmental Protection Service Tameside MBC Council Offices, (2008). [Online] available: http://www.tameside.gov.uk/airquality

Fauziah, Ahmad; Ahmad Shukri Yahaya & Mohd Ahmadullah Farooqi. (2006), Characterization and Geotechnical Properties of Penang Residual Soils with Emphasis on Landslides, American Journal of Environmental Sciences 2 (4): 121-128

Fukushima, H.; Toratani, M.; Yamamiya, S. & Mitomi, Y. (2000). Atmospheric correction algorithm for ADEOS/OCTS acean color data: performance comparison based on ship and buoy measurements. Adv. Space Res, Vol. 25, No. 5, 1015-1024

Fundamentals of Remote Sensing, [Online] available: http://www.ccrs.nrcan.gc.ca/resource/tutor/fundam/pdf/fundamentals_e.pdf

Jensen, J. R. (2006), Remote Sensing of the Environment: An Earth Resource Perspective, 2nd Ed., Upper Saddle River, NJ: Prentice Hall. [Online] available:, http://www.cas.sc.edu/geog/Rsbook/Lectures/Rse/index.html

Kaufman,; Y. J., Tanr, D. C.; Gordon, H. R.; Nakajima, T.; Lenoble, J.; Frouins, R.; Grassl, H.; Herman, B. M..; King, M. D. & Teillet, P. M. (1997). Passive remote sensing of tropospheric aerosol and atmospheric correction for the aerosol effect. Journal of Geophysical Research, 102 (D14):16,815-16,830

Liu, C. H.; Chen, A. J. ^ Liu, G. R. (1996). An image-based retrieval algorithm of aerosol characteristics and surface reflectance for satellite images, International Journal Of Remote Sensing, 17 (17), 3477-3500

King, M. D.; Kaufman, Y. J.; Tanre, D. & Nakajima, T. (1999). Remote sensing of tropospheric aerosold form space: past, present and future, Bulletin of the American Meteorological society, 2229-2259

Penner, J. E.; Zhang, S. Y.; Chin, M.; Chuang, C. C.; Feichter, J.; Feng, Y.; Geogdzhayev, I. V.; Ginoux, P.; Herzog, M.; Higurashi, A.; Koch, D.; Land, C.; Lohmann, U.; Mishchenko, M.; Nakajima, T.; Pitari, G.; Soden, B.; Tegen, I. & Stowe, L. (2002). A Comparison of Model And Satellite-Derived Optical Depth And Reflectivity. [Online} available: http://data.engin.umich.edu/Penner/paper3.pdf

Popp, C.; Schläpfer, D.; Bojinski, S.; Schaepman, M. & Itten, K. I. (2004). Evaluation of Aerosol Mapping Methods using AVIRIS Imagery. R. Green (Editor), 13th Annual JPL Airborne Earth Science Workshop. JPL Publications, March 2004, Pasadena, CA, 10

Quaidrari, H. dan Vermote, E. F. (1999). Operational atmospheric correction of Landsat TM data, Remote Sensing Environment, 70: 4-15.

Retalis, A.; Sifakis, N.; Grosso, N.; Paronis, D. & Sarigiannis, D. (2003). Aerosol optical thickness retrieval from AVHRR images over the Athens urban area, [Online] available: http://sat2.space.noa.gr/rsensing/documents/IGARSS2003_AVHRR_Retalisetal_web.pdf

UNEP Assessment Report, Part I: The South Asian Haze: Air Pollution, Ozone and Aerosols, [Online] available: http://www.rrcap.unep.org/issues/air/impactstudy/Part%20I.pdf

Ung, A.; Weber, C.; Perron, G.; Hirsch, J.; Kleinpeter, J.; Wald, L. & Ranchin, T. (2001a). Air Pollution Mapping Over A City – Virtual Stations And Morphological Indicators. Proceedings of 10th International Symposium "Transport and Air Pollution" September 17 - 19, 2001 – Boulder, Colorado

Ung, A.; Wald, L.; Ranchin, T.; Weber, C.; Hirsch, J.; Perron, G. & Kleinpeter, J. (2001b). Satellite data for Air Pollution Mapping Over A City- Virtual Stations, Proceeding of the 21th EARSeL Symposium, Observing Our Environment From Space: New Solutions For A New Millenium, Paris, France, 14 – 16 May 2001, Gerard Begni Editor, A., A., Balkema, Lisse, Abingdon, Exton (PA), Tokyo, pp. 147 – 151, [Online] available: http://www-cenerg.cma.fr/Public/themes_de_recherche/teledetection/title_tele_air/title_tele_air_pub/satellite_data_for_t

Sifakis, N. & Deschamps, P.Y. (1992). Mapping of air pollution using SPOT satellite data, Photogrammetric Engineering & Remote Sensing, 58(10), 1433 – 1437

Sifakis, N. I.; Soulakellis, N. A. & Paronis, D. K. (1998). Quantitative mapping of air pollution density using Earth observations: a new processing method and application to an urban area, International Journal Remote Sensing, 19(17): 3289 – 3300

The Digital Awakening-Haze in Penang, (2009). [Online] available: http://www.petertan.com/blog/2005/08/12/haze-in-penang/

The Digital Awakening--Haze in Penang Update - 10.48am, [Online] available: http://www.petertan.com/blog/2005/08/13/haze-in-penang-update-1048am/

Vincentchow, (2009). Available Online: http://www.vincentchow.net/289/haze-in-malaysia

Vermote, E. & Roger, J. C. (1996). Advances in the use of NOAA AVHRR data for land application: Radiative transfer modeling for calibration and atmospheric correction, Kluwer Academic Publishers, Dordrecht/Boston/London, 49-72

Vermote, E.; Tanre, D.; Deuze, J. L.; Herman, M. & Morcrette, J. J. (1997). 6S user guide Version 2, Second Simulation of the satellite signal in the solar spectrum (6S), [Online] available: http://www.geog.tamu.edu/klein/geog661/handouts/6s/6smanv2.0_P1.pdf

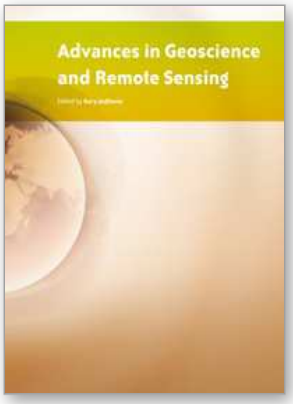

Advances in Geoscience and Remote Sensing

Edited by Gary Jedlovec

ISBN 978-953-307-005-6

Hard cover, 742 pages

Publisher InTech

Published online 01, October, 2009

Published in print edition October, 2009

Remote sensing is the acquisition of information of an object or phenomenon, by the use of either recording or real-time sensing device(s), that is not in physical or intimate contact with the object (such as by way of aircraft, spacecraft, satellite, buoy, or ship). In practice, remote sensing is the stand-off collection through the use of a variety of devices for gathering information on a given object or area. Human existence is dependent on our ability to understand, utilize, manage and maintain the environment we live in - Geoscience is the science that seeks to achieve these goals. This book is a collection of contributions from world-class scientists, engineers and educators engaged in the fields of geoscience and remote sensing.

How to reference

In order to correctly reference this scholarly work, feel free to copy and paste the following:

H. S. Lim, M. Z. MatJafri, K. Abdullah and C. J. Wong (2009). Air Pollution Determination Using Remote Sensing Technique, Advances in Geoscience and Remote Sensing, Gary Jedlovec (Ed.), ISBN: 978-953-307-005-6, InTech, Available from: http://www.intechopen.com/books/advances-in-geoscience-and-remote-sensing/air-pollution-determination-using-remote-sensing-technique

INTECH
open science | open minds

InTech Europe
University Campus STeP Ri
Slavka Krautzeka 83/A
51000 Rijeka, Croatia
Phone: +385 (51) 770 447
Fax: +385 (51) 686 166
www.intechopen.com

InTech China
Unit 405, Office Block, Hotel Equatorial Shanghai
No.65, Yan An Road (West), Shanghai, 200040, China
中国上海市延安西路65号上海国际贵都大饭店办公楼405单元
Phone: +86-21-62489820
Fax: +86-21-62489821

© 2009 The Author(s). Licensee IntechOpen. This chapter is distributed under the terms of the Creative Commons Attribution-NonCommercial-ShareAlike-3.0 License, which permits use, distribution and reproduction for non-commercial purposes, provided the original is properly cited and derivative works building on this content are distributed under the same license.